CORE-BASED PETROPHYSICAL ROCK CLASSIFICATION BY QUANTIFYING PORE-SYSTEM ORTHOGONALITY WITH A BIMODAL GAUSSIAN DENSITY FUNCTION

Chicheng Xu and Carlos Torres-Verdín
The University of Texas at Austin

This paper was prepared for presentation at the International Symposium of the Society of Core Analysts held in Napa Valley, California, USA, 16-19 September, 2013

ABSTRACT

Tight-gas sandstones exhibit large petrophysical variability due to complex pore structure resulting from diagenesis. Consequently, conventional rock classification schemes that rely solely on hydraulic radius to rank tight-gas sandstones are inadequate to capture all petrophysical variations. New methods for describing complex pore systems are necessary for more reliable petrophysical rock typing. We compare two distribution functions, namely Gaussian and Thomeer's derivative, to assess their reliability to model pore-size distributions analytically from mercury injection capillary pressure data. Our comparative study shows that Gaussian density functions are effective to describe the pore system and provide analytical representations to calculate macroscopic petrophysical properties. Based on the study, we introduce a bimodal Gaussian density function to characterize pore-size distributions in terms of incremental pore volume fraction versus logarithmic pore-throat radius. This quantitative pore-system description underlies a new petrophysical rock typing method which defines petrophysical orthogonality between two pore systems using all relevant pore-system attributes based on the "bundle of capillary tubes" model. We test the new method with both routine and special core laboratory data acquired in a key-study well in the Bossier tight-gas sand field located in the East Texas Basin. The field case confirms that the new rock classification scheme properly captures petrophysical trends and variability.

INTRODUCTION

Rock typing is routinely performed with porosity and permeability data (Corbett and Potter, 2004) and mercury injection capillary pressure curves (MICP) (Pittman, 1992). G.E. Archie (1950) noted that petrophysical rock typing should be based on the associated pore-size distribution, which links the rock's static and dynamic petrophysical properties. Different forms of pore-size distribution from various data sources have been documented and compared in previous publications (Basan et al., 1997). In this paper, pore-size distribution refers to incremental pore volume fraction versus logarithmic pore-throat radius, which is typically calculated from MICP curves using derivation method (Lenormand, 2003; Peters, 2012). Several authors (Clerke, 2009; Gao et al., 2011) documented their experience on using multiple Thomeer's hyperbolas (1960) to fit MICP

curves when describing complex carbonate rock pore systems. This procedure implicitly invokes the derivative of Thomeer's hyperbolas (referred to as Thomeer's derivative) as the pore-size distribution function. Xu and Torres-Verdín (2013a) introduced a bimodal Gaussian density function to characterize pore-size distributions from MICP data, which gives rise to six attributes of interpretable petrophysical meaning. An important remaining piece of work is to combine all relevant attributes to define the petrophysical dissimilarity (conceptualized as petrophysical orthogonality) between pore systems for petrophysically consistent rock classification.

In this paper, we first compare the reliability of Gaussian and Thomeer's derivative in describing complex pore systems. We then use bimodal Gaussian density functions to quantify complex pore systems in terms of pore volume, pore connectivity, and pore-size uniformity. Six attributes for each density function are estimated and interpreted for petrophysical meaning and subsequently integrated to assess petrophysical orthogonality between two pore systems. We introduce a new petrophysical rock typing method by clustering the orthogonality matrices after fitting MICP data, which provides good ranking of reservoir quality and enforces petrophysical consistency among all static and dynamic petrophysical properties. The new classification method is verified with field data acquired in the Bossier tight-gas sand reservoir located in the East Texas Basin.

METHODS

Bimodal Gaussian Pore-Size Distribution. Pore-throat size is often quantified on a logarithmic scale due to its wide variability across several orders of magnitude. Therefore, all Gaussian density functions in this paper treat the distribution of pore-throat size on a logarithmic scale (i.e., log-normal distribution). A bimodal Gaussian density function is expressed as

$$p(\log R; w_1, \log\mu_1, \log\sigma_1; w_2, \log\mu_2, \log\sigma_2) =$$

$$w_1 \frac{1}{\sqrt{2\pi}\log\sigma_1} e^{-\frac{(\log R-\log\mu_1)^2}{2(\log\sigma_1)^2}} + w_2 \frac{1}{\sqrt{2\pi}\log\sigma_2} e^{-\frac{(\log R-\log\mu_2)^2}{2(\log\sigma_2)^2}}, \quad (1)$$

where R is pore-throat radius in μm, w_1 and w_2 are weighting coefficients for each Gaussian mode, $\log\mu_1$ and $\log\mu_2$ are the mean values of logarithmic pore-throat radius, and $\log\sigma_1$ and $\log\sigma_2$ are the corresponding standard deviations of logarithmic pore-throat radius. The petrophysical interpretation of these attributes is summarized as follows:

> **Pore Volume:** w_1 and w_2 are fractions of pore volume connected by large and small logarithmic pore-throat radius modes, respectively; w_1 correlates with residual non-wetting phase saturation during imbibition, while w_2 correlates with irreducible wetting-phase saturation during drainage (Mohanty and Salter, 1982).
> **Pore Connectivity:** $\log\mu_1$ and $\log\mu_2$ are mean values of large and small logarithmic pore-throat radius modes, respectively; large values indicate better pore connectivity as well as permeability.
> **Pore-Size Uniformity:** $\log\sigma_1$ and $\log\sigma_2$ are standard deviations of large and small logarithmic pore-throat radius modes, which describe the uniformity of "capillary

tube sizes" (Childs and Collis-George, 1950). A larger value of standard deviation of pore-throat radius indicates possibly lower sorting of tube sizes, therefore higher tortuosity of the pore network.

Xu and Torres-Verdín (2013a) introduced both differentiation and inversion methods to calculate bimodal Gaussian density functions from MICP data. The inversion method is preferred because it generates stable and smooth pore-size distribution functions.

Comparison with Thomeer's Derivative. Thomeer's hyperbola is expressed as

$$S_{hg} = 1 - S_w = e^{-G/(\log P_c - \log P_d)}, \quad (2)$$

where S_{hg} is mercury saturation and S_w is the corresponding wetting phase saturation at capillary pressure P_c, G is pore geometrical factor reflecting the distribution of pore throats and their associated pore volume, and P_d is the extrapolated displacement or entry pressure. The derivative of Thomeer's hyperbola is used implicitly as pore-size distribution function, given by

$$f(\log P_c, G, P_d) = \frac{dS_w}{d(\log P_c)} = \frac{G}{\log P_c - \log P_d} \times e^{-G/(\log P_c - \log P_d)}. \quad (3)$$

Figure 1 shows an example of fitting MICP data using Gaussian and Thomeer's derivative as pore-size distribution functions. Although both functions fit the MICP curve, the parameters in the Gaussian density function relate more directly and intuitively to pore-system attributes than the parameters included in Thomeer's derivative. Noteworthy is that Thomeer's model has the advantage to define a threshold pressure. This can also be achieved by introducing a cut-off in pore-throat size in the Gaussian model.

Petrophysical Rock Classification with Pore-System Orthogonality. Xu and Torres-Verdín (2013b) quantified the petrophysical orthogonality between two pore systems as

$$ORT_{1,2} = \log(\frac{\phi_1}{\phi_2}) + 2\log(\frac{\mu_1}{\mu_2}) - 0.5\log(\frac{\sigma_1}{\sigma_2}), \quad (4)$$

where $ORT_{1,2}$ quantifies orthogonality between two unimodal Gaussian pore-size distributions. A positive orthogonality indicates that pore system No. 1 has better reservoir quality than pore system No. 2. Under this mathematical formulation, petrophysical orthogonality has the following properties:

(i) the orthogonality between two identical pore systems is zero;

(ii) $$ORT_{1,3} = ORT_{1,2} + ORT_{2,3}, \quad (5)$$

where subscripts 1, 2, and 3 represent three pore systems. After fitting all MICP curves (total number = N) with Eq. (1), we calculate the petrophysical orthogonality between each core sample pair using Eq. (4) for both large and small pore-size modes, which are described in the form of NxN matrices. Diagonal elements of orthogonality matrices are all zero according to (i). The matrices rank all core samples in terms of reservoir quality, whereby they become suitable for petrophysical rock classification. We apply the dissimilarity matrix clustering technique (Hahsler and Hornik, 2011) to orthogonality matrices and classify MICP core samples into rock types with descending reservoir quality.

FIELD CASE

We test the new method with a set of core data from the Bossier tight-gas sand formation, Upper Jurassic Cotton Valley Group in the East Texas Basin. Comprehensive core data from a key-study well was acquired for high-resolution petrophysical reservoir description (Rushing et al., 2008). Routine core porosity and permeability measurements were performed on more than 100 core plugs, which exhibit low porosity ranging from 2 to 10 p.u. and low permeability ranging from 0.001 to 1 mD. In addition, high-pressure MICP (0 – 60,000 psi) and NMR measurements were also measured on 20 preserved core plugs covering different depositional facies from a continuous full-diameter whole core.

Figures 2a and 2b show the MICP curves the MICP-derived pore-size distributions ranked with rock types classified with the clustering orthogonality matrices. All rock types exhibit a dominant Gaussian pore-size distribution and a tail of small Gaussian pore-size distribution. We use the classification results obtained with clustering orthogonality matrices to color-code the porosity-permeability crossplot (Fig. 2c). Clear porosity-permeability trends are observed for all rock types. Figures 2d-2g show the core NMR T_2 spectra grouped by rock types and Fig. 2h shows the crossplot of permeability and T2LM color-coded by rock types. Generally, T_2 peak locations move leftward (lower T_2) as the rock type number increases (overall reservoir quality decreases). The consistent description of rock types with different data confirms that the defined pore-system orthogonality provide a reliable petrophysical ranking criterion.

CONCLUSIONS

We introduced a bimodal Gaussian density function to describe complex pore systems analytically in terms of pore volume, pore connectivity, and pore-size uniformity. A new concept, referred to as pore-system orthogonality, was introduced to quantify petrophysical dissimilarity between two pore systems, which takes into account all relevant pore-system attributes, including pore volume, pore connectivity, and pore-size uniformity. Rock classification via clustering orthogonality matrices enables consistent reservoir quality ranking in all petrophysical data domains, including porosity-permeability trends, pore-size distribution, mercury injection capillary pressure, and core NMR T_2 spectra. A test of the new method on twenty core samples from the Bossier tight-gas sandstones, East Texas, verified the reliability of the petrophysical ranking method.

ACKNOWLEDGMENTS

We would like to thank Anadarko Petroleum Cooperation for providing the field data used for analysis and verification. The work reported in this paper was funded by The University of Texas at Austin's Research Consortium on Formation Evaluation, jointly sponsored by Afren, Anadarko, Apache, Aramco, Baker-Hughes, BG, BHP Billiton, BP, Chevron, China Oilfield Services, LTD., ConocoPhillips, ENI, ExxonMobil, Halliburton, Hess, Maersk, Marathon Oil Corporation, Mexican Institute for Petroleum, Nexen, ONGC, OXY, Petrobras, PTTEP, Repsol, RWE, Schlumberger, Shell, Statoil, Total, Weatherford, Wintershall and Woodside Petroleum Limited.

REFERENCES

1. Archie, G.E., 1950, Introduction to Petrophysics of Reservoir Rocks, *AAPG Bulletin*, 34(5):943-961.
2. Basan, P.B., Lowden, B.D., Whattler, P.R., and Attard, J., 1997, Pore-Size Data in Petrophysics: A Perspective on the Measurement of Pore Geometry, Geological Society, London, Special Publications, 122:47-67.
3. Childs, E.C. and Collis-George, N., 1950, The Permeability of Porous Materials. *Proceedings of the Royal Society A*, 201(1066):392–405.
4. Clerke, E.A., 2009, Permeability, Relative Permeability, Microscopic Displacement Efficiency, and Pore Geometry of M_1 Bimodal Pore Systems in Arab D Limestone, *SPE Journal*, 14(3):524-531.
5. Corbett, P. W. M., and Potter, D. K., 2004, Petrotyping – a Basemap and Atlas for Navigating through Permeability and Porosity Data for Reservoir Comparison and Permeability Prediction, Paper SCA2004-30 presented at International Symposium of the Society of Core Analysts, Abu Dhabi, U.A.E., October 5 – 9.
6. Gao, B., Wu, J.H., Chen, S.H., Kwak, H., and Funk, J., 2011, New Method for Predicting Capillary Pressure Curves from NMR Data in Carbonate Rocks, *SPWLA 52nd Annual Logging Symposium*, Colorado Springs, Colorado, May 14 – 18.
7. Hahsler, M., and Hornik K., 2011, Dissimilarity Plots: A Visual Exploration Tool for Partitional Clustering, *Journal of Computational and Graphical Statistics*, 20(2): 335-354.
8. Lenormand, R., 2003, Interpretation of Mercury Injection Curves to Derive Pore Size Distribution, Paper SCA2003-52 presented at International Symposium of the Society of Core Analysts, Pau, France, September 21 – 24.
9. Mohanty, K.K. and Salter, S.J., 1982, Multiphase Flow in Porous Media: II. Pore-Level Modeling, paper SPE 11018 presented at SPE Annual Technical Conference and Exhibition, New Orleans, Louisiana, September 26-29.
10. Peters, E.J., 2012, Advanced Petrophysics – Volumes 1 and 2. Greenleaf Book Group, Austin.
11. Pittman, E.D. 1992, Relationship of Porosity and Permeability to Various Parameters Derived from Mercury Injection-Capillary Pressure Curves for Sandstone, AAPG Bulletin, 76 (2): 191 -198.
12. Rushing, J.A., Newsham, K.E., and Blasingame T.A., 2008, Rock Typing – Keys to Understanding Productivity in Tight Gas Sands, *Paper SPE 114164 presented at SPE Unconventional Reservoirs Conference*, Keystone, Colorado, February 10-12.
13. Thomeer, J.H.M., 1960, Introduction of a Pore Geometrical Factor Defined by the Capillary Pressure Curve, *Journal of Petroleum Technology*, 12(3): 73-77.
14. Xu, C. andTorres-Verdín, C., 2013a, Pore System Characterization and Petrophysical Rock Classification Using a Bimodal Gaussian Density Function, *Mathematical Geosciences*, in press. (DOI: 10.1007/s11004-013-9473-2).
15. Xu, C. and Torres-Verdín, C., 2013b, Petrophysical Rock Classification in the Cotton Valley Tight Gas Sand Reservoir with a Clustering Pore-System Orthogonality Matrix, *SEG Interpretation* (submitted for review).

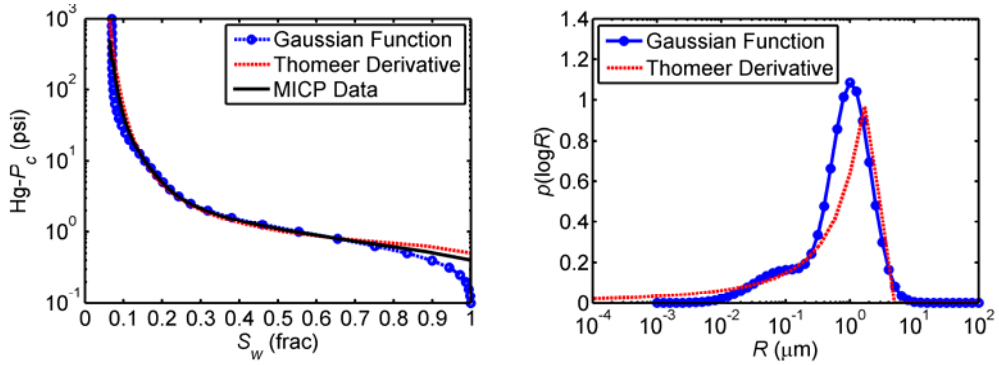

Figure 1: Comparison of using a Gaussian density function and Thomeer's derivative to model pore-size distributions from MICP data. Right panel: MICP modeling; Left panel: pore-size distribution modeling.

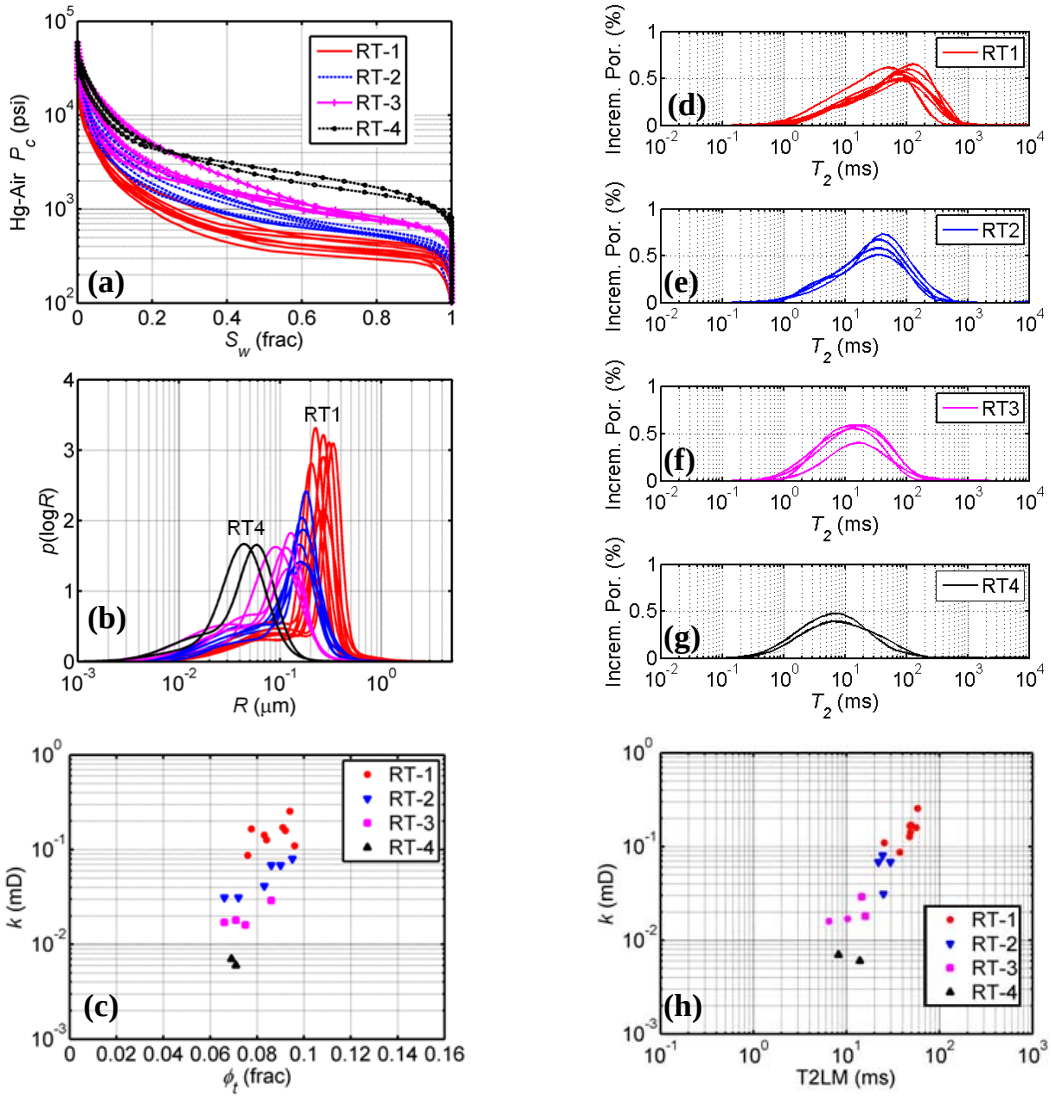

Figure 2: Ranking of rock types in different data forms with pore-system orthogonality.